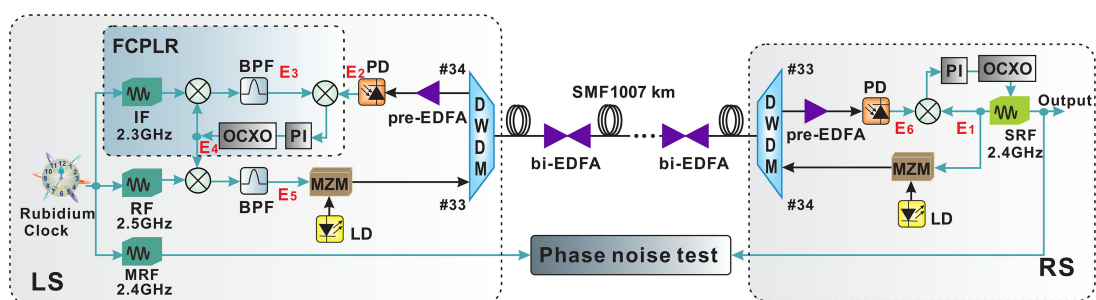


Ultrastable Long-Haul Fiber-Optic Radio Frequency Transfer Based on Dual-PLL

Volume 13, Number 1, February 2021

Chenxia Liu
Jianming Shang
Zhuoze Zhao
Hao Gao
Jinting Cong
Junjie Shi
Bin Luo
Xing Chen
Song Yu



DOI: 10.1109/JPHOT.2020.3043263

Ultrastable Long-Haul Fiber-Optic Radio Frequency Transfer Based on Dual-PLL

Chenxia Liu, Jianming Shang, Zhuoze Zhao, Hao Gao, Jinting Cong, Junjie Shi, Bin Luo, Xing Chen, and Song Yu

State Key Laboratory of Information Photonics and Optical Communications, Beijing
University of Posts and Telecommunications, Beijing 100876, China

DOI:10.1109/JPHOT.2020.3043263

This work is licensed under a Creative Commons Attribution 4.0 License. For more information, see <https://creativecommons.org/licenses/by/4.0/>

Manuscript received October 22, 2020; revised December 4, 2020; accepted December 4, 2020. Date of publication December 8, 2020; date of current version January 6, 2021. This work was supported in part by the National Natural Science Foundation under Grants 61901046, 61531003, 61701040, and 61427813, in part by the Fundamental Research Funds for the Central Universities under Grants 2019XD-A18 and 2019PTB-004, and in part by Youth Research and Innovation Program of BUPT. Corresponding author: Bin Luo (e-mail: luobin@bupt.edu.cn).

Abstract: In this paper, we demonstrate ultrastable radio-frequency (RF) transfer over long-haul optical fiber link. Our stabilized RF transfer technique is based on high-performance dual phase locked loops (dual-PLL) configuration which improves signal to noise ratio (SNR) of the round trip transmitted signals. At the local site, the frequency conversion phase-lock receiver (FCPLR) accomplishes high-quality phase tracking of the RF signal which is transmitted after long distance optical fiber link. The low phase noise signal generated by FCPLR is passively mixed with a local reference signal to realize phase conjugation. Through advisable frequency design, there is no residual RF leakage and nonlinear effect of frequency mixing. Another PLL incorporating a high-quality cleanup oscillator is located at the remote site that favourably improves short-term instability of our transmission system. In our experiment, stabilized 2.4 GHz RF signal transfer over a 1007 km optical fiber link is demonstrated without any electric relay system, and the transmission system achieves a fractional frequency instability of 8.20×10^{-14} @1 s and 7.87×10^{-17} @10 000 s.

Index Terms: Frequency instability, optical fiber link, radio frequency transfer.

1. Introduction

In modern astronomy, the interferometric arrays, like Square Kilometre Array (SKA), Atacama Large Millimeter Array (ALMA) and next generation Very Large Array (ngVLA), have been expected to tackle many outstanding scientific questions [1]–[3]. These arrays require coherent frequency reference signals at each antenna in the array to achieve phase coherence for performing interferometry and beamforming [4]. Higher sensitivity and spatial resolution of the arrays benefit from the implementation of very long baselines (~ 1000 km) [3]. Thus, high stable frequency reference signals transfer over long distance become essential in the field of radio astronomy. The still growing infrastructure of installed optical fiber links and their good transmission properties give much place to high stable frequency distribution [5]–[16]. As any other transmission medium, optical fiber links display some fluctuations of the propagation delay, which is caused by temperature variations and mechanical vibrations. Further, these environmental factors result in phase fluctuations of the transmitted signals. The excess phase noise requires to be detected and subsequently compensated in order to stably transfer the frequency reference signal via long-haul fiber link.

Many stable frequency dissemination schemes have been proposed and demonstrated, which include optical frequency transmission, optical frequency comb transmission and radio or microwave frequency transmission [5]–[26]. Among these typical solutions, optical frequency and comb transfer provide better short-term instabilities than radio or microwave frequency transfer using amplitude modulation. One of the leading causes is that the modulated optical signal transfer makes use of limited modulation index, whereas optical frequency and comb have higher signal to noise ratio (SNR) when performing heterodyne beat or direct photodetection [27]. Nevertheless, optical frequency transfer offers very little flexibility. The remote user needs optical frequency comb to download radio or microwave frequency signals, which are required in the aforementioned applications. In consideration of complexity and cost of the optical frequency comb, stable radio frequency (RF) transfer over fiber becomes more practical and have been widely demonstrated [13]–[24]. There are two basic limitations in long-haul fiber-optic frequency transfer systems [28]. One of the two is a distance limitation set by SNR of the received signal, which affects phase jitter of the transmitted signal [29]. Ultimately, it directly determines the transfer instability, expressed usually as Allan deviation (ADEV) [30]. The stable RF transfer based on passive phase correction method is summarized by Pan et al. which has a relatively simple structure without any tunable device [31]. But the passive phase correction method could not remedy the SNR degradation and usually result in limited transmission distance and frequency stability [20]–[24]. In the previous solutions, cascaded systems are applied which extend the transmission length to a few hundred kilometers [11], [16], [17]. However, the transfer instability degrades \sqrt{N} times in a cascaded system with N stages [11].

In this paper, unlike the aforementioned passive phase correction method, the active dual phase locked loops (dual-PLL) configuration is designed in our ultrastable fiber-optic RF transfer system. At the local site (LS), the PLL acts as a frequency conversion phase-lock receiver (FCPLR) and improves the SNR of the output signal after the phase-lock receiving process. Two auxiliary RF signal sources are employed and there is no RF leakage and nonlinear effect of frequency mixing. At the remote site (RS), the PLL incorporating a high-quality cleanup oscillator not only guarantees the SNR of the round trip transmitted signal, but also maintains enough short-term stability during the round-trip transmission time when the PLL is locked. As a consequence, the short-term instability of our transmission system is improved. The proposed scheme is tested over 1007 km optical fiber link with only one stage system. Ten low noise homemade bi-directional erbium doped fiber amplifier (bi-EDFA) modules and two low noise unidirectional pre-EDFAs are utilized to compensate the fiber loss which is 245.2 dB in total. The proposed scheme compensates for fiber-induced phase fluctuations on a time scale that is longer than the fiber round-trip time (about 10 ms for a 1007 km system). Here, we will show a comprehensive work corresponding to our previous outcome [32]. Among the schemes mentioned above, Wang et al. achieved a good ADEV result with 7×10^{-15} @1 s and 4×10^{-18} @10 000 s and Liu et al. accomplished stable RF transfer via 430 km underground optical fiber link [5], [16]. Comparably, the measured fractional frequency instability(ADEV) of our transmission system over 1007 km fiber link is 8.20×10^{-14} @1 s and 7.87×10^{-17} @10 000 s.

2. Principle

The schematic diagram of our stable RF transmission system is shown in Fig. 1. Our goal is to synchronize the slave radio frequency signal (SRF), ω_{SRF} , with the master radio frequency reference signal (MRF), ω_{MRF} , which is locked to an atomic clock at the LS. Our phase noise cancellation scheme can be understood as follows. The 2.4 GHz SRF generated at the RS can be denoted as

$$E_1 = \cos(\omega_{SRF}t + \varphi_{SRF}), \quad (1)$$

where ω_{SRF} and φ_{SRF} are its angular frequency and initial phase, respectively. It is intensity modulated on the optical carrier and transmitted to LS via single-mode fiber (SMF). Signal detected

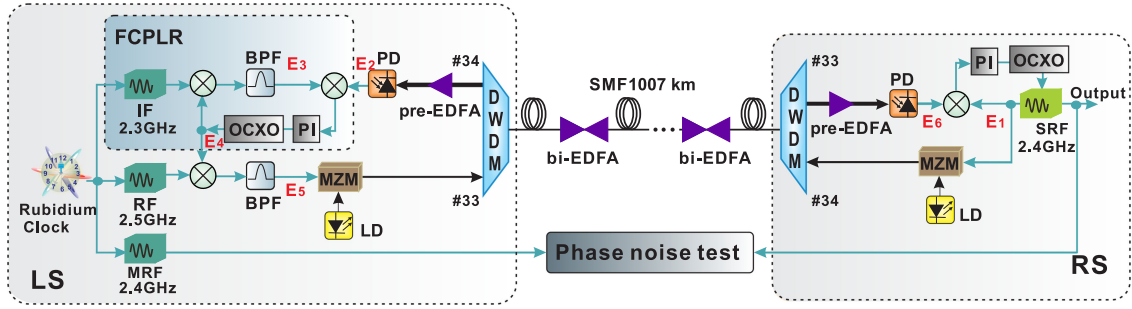


Fig. 1. Schematic diagram of the stable 2.4 GHz RF frequency dissemination scheme. SMF: single-mode fiber. BPF: band pass filter. PD: photo-detector. LD: laser diode. OCXO: oven controlled crystal oscillator. PI: proportional integral controller. IF: intermediate frequency signal generator. RF: radio frequency signal generator. MRF: master radio frequency signal generator. SRF: slave radio frequency signal generator. DWDM: dense wavelength division multiplexing. bi-EDFA: bi-directional erbium-doped fiber amplifier. FCPLR: frequency conversion phase-lock receiver. LS: local site. RS: remote site.

by the photo detector (PD) is

$$E_2 = \cos(\omega_{SRF}t + \varphi_{SRF} + \varphi_{fiber}), \quad (2)$$

where φ_{fiber} is the phase fluctuation corresponding to the entire optical fiber link and ω_{SRF} . In order to improve the SNR of the phase conjugate signal which is to be transmitted to RS, we adopt a high performance PLL during the frequency mixing process. At the LS, an auxiliary 2.3 GHz intermediate frequency signal (IF), ω_{IF} , is employed and mixed with the 100 MHz signal from a high precision oven controlled crystal oscillator (OCXO). After a band pass filter (BPF), the sum frequency signal E_3 can be expressed as

$$E_3 = \cos(\omega_{IF}t + \omega_0t + \varphi_{IF} + \varphi_0), \quad (3)$$

where ω_{IF} and φ_{IF} are angular frequency and initial phase of the auxiliary 2.3 GHz signal, and ω_0 and φ_0 are angular frequency and initial phase of the 100 MHz signal. Signal E_2 is phase discriminated with the 2.4 GHz sum frequency signal E_3 , and the phase error signal is fed back to OCXO through a proportional integral controller (PI). Hence, phase of this photodetected signal is precisely tracked when the PLL is locked. Output of the OCXO can be written as

$$E_4 = \cos(\omega_{SRF}t - \omega_{IF}t + \varphi_{SRF} + \varphi_{fiber} - \varphi_{IF}). \quad (4)$$

The phase noise of the OCXO is not included here. Because OCXO has excellent short-term stability, which corresponds to the remarkable phase noise at far end of the frequency domain. The phase noise of OCXO (-150 dBc/Hz@1 kHz, -165 dBc/Hz@10 kHz) is superior to that of the rubidium clock (-145 dBc/Hz@1 kHz, -150 dBc/Hz@10 kHz). As a consequence, it can maintain sufficient stability on the time scale of round-trip transmission like the clock. Then, a 2.4 GHz phase conjugate signal E_5 is obtained, where one branch of OCXO output is frequency up converted by being mixed with another auxiliary 2.5 GHz RF signal, ω_{RF} . Signal E_5 can be expressed as

$$E_5 = \cos(\omega_{RF}t + \omega_{IF}t - \omega_{SRF}t + \varphi_{RF} + \varphi_{IF} - \varphi_{SRF} - \varphi_{fiber}). \quad (5)$$

After this phase conjugate signal is transmitted to RS, the returning noise term φ_{fiber} algebraically cancels the phase-conjugate fiber-optic noise term. At the RS, the signal after PD is

$$E_6 = \cos(\omega_{RF}t + \omega_{IF}t - \omega_{SRF}t + \varphi_{RF} + \varphi_{IF} - \varphi_{SRF}). \quad (6)$$

With fiber-induced phase variations compensated, the signal E_6 is then mixed with signal E_1 and regenerated via the remote PLL. After the PLL is locked, signal E_1 becomes

$$E_1 = \cos[(\omega_{RF}t + \omega_{IF}t)/2 + (\varphi_{RF} + \varphi_{IF})/2]. \quad (7)$$

TABLE 1
Details of the 1007 Km Fiber Link

No.	1	2	3	4	5	6	7	8	9	10	11	Total
Length [km]	91.7	111.5	71.4	88.9	88.8	91.1	107.6	90.1	89.7	90.4	86.1	1007
Attn. [dB]	23.6	24.6	22.9	19.0	22.8	23.5	23.6	23.5	22.6	22.0	17.1	245.2

Due to the relationship of $2\omega_{MRF} = \omega_{RF} + \omega_{IF}$, a 2.4 GHz MRF at LS is generated and used to measure the frequency transmission instability of our system. Three phase-locked dielectric resonant oscillators (PDRO) act as frequency synthesizers at LS which are all locked to the atomic clock. Here, we should note that the phases of three signal generators have the relationship of $2\varphi_{MRF} = \varphi_{RF} + \varphi_{IF} + \xi$, where ξ is constant. As a consequence, the output of the SRF generator can be expressed as

$$E_1 = \cos(\omega_{MRF}t + \varphi_{MRF} - \xi/2). \quad (8)$$

We can see that a stable RF signal is generated at RS which is referenced to MRF. The fractional frequency instability of our stabilized 2.4 GHz signal transmission system can be measured by comparing the phase of SRF to that of the MRF through the phase noise test devices.

3. Experimental Setup and Results

In our experiment, the length of optical fiber link is 1007 km, and the fiber loss is 245.2 dB in total. Table 1 gives the length of the transmission fiber which contains 590 km G.652 SMF and 417 km G.655 SMF. The homemade bi-directional EDFA includes two unidirectional EDFAs, which are used to amplify the power of optical signals in the inverse directions. Two wavelength-division multiplexers (WDMs) are placed at both ends of the bi-EDFA to increase the isolation of different wavelength channels and prevent the reflection light signal from being amplified. In order to obtain high SNR detection, one low noise unidirectional pre-EDFA is placed before each of the two PDs to amplify the optical signal. The optical power injected into each PD is guaranteed to be -1 dBm. Table 1 shows the details of the 1007 km fiber link in our lab. Proper dispersion compensation fiber (DCF) is contained to reduce the time delay asymmetry of the optical path of the two directions caused by group velocity dispersion (GVD). The effect of backscattering is efficiently suppressed by using two different wavelengths at LS and RS, channel #33 (1550.92 nm) and channel #34 (1550.12 nm). The bandwidth of PI servo is limited to frequency less than 100 Hz, which is the inverse optical-transmission round-trip time [33]. The PDROs used in our experiment have ultral low phase noises, which are -102 dBc/Hz@100 Hz, -126 dBc/Hz@1 kHz, and -131 dBc/Hz@100 kHz. The high stable and low noise OCXO (MORION MV218) included both in the local and remote PLL can maintain sufficient stability on the time scale of round-trip transmission (~ 10 ms). Importantly, SNR of the transferred signal is deteriorated severely due to the attenuation of long-haul fiber link and several noises in the transmission system. The SNR degradation caused by tandem optical amplifiers has been published in textbooks [34]. After transmitted via the fiber link, the detected RF signal power is

$$P_{s-total} = e^2 \left(\langle n_{in} \rangle \prod_{i=1}^N L_i G_i \right)^2 m^2 / 2, \quad (9)$$

where e is electron charge, $\langle n_{in} \rangle$ is mean number of photons per unit time at the optical fiber input, L is the SMF and DCF loss of the optical amplifier spacing, G is gain of each EDFA, N is the total number of the EDFAs and m is modulation index. Then, total power of the dominant noises

accumulated in the transmission process is

$$\begin{aligned}
 P_{n-total} = & 2e^2 n_{RIN} \left(\langle n_{in} \rangle \prod_{i=1}^N L_i G_i \right)^2 B + 2e^2 n_{sp} m_t \Delta f \left[\sum_{i=1}^N (G_i - 1) \prod_{j=i+1}^N L_j G_j \right] B \\
 & + 4e^2 n_{sp} \left(\langle n_{in} \rangle \prod_{i=1}^N L_i G_i \right) \left[\sum_{i=1}^N (G_i - 1) \prod_{j=i+1}^N L_j G_j \right] B \\
 & + 2e^2 n_{sp}^2 m_t \Delta f \left[\sum_{i=1}^N (G_i - 1) \prod_{j=i+1}^N L_j G_j \right]^2 B + 2e^2 \left(\langle n_{in} \rangle \prod_{i=1}^N L_i G_i \right) B + 4kTB/R_L,
 \end{aligned} \tag{10}$$

where n_{RIN} is relative intensity noise (RIN) of the signal light itself, B is the electric filter bandwidth, n_{sp} is the population inversion parameter of the optical amplifier, m_t is the aggregate number of polarizations in the amplification medium, Δf is the optical filter bandwidth, k is Boltzmann's constant, T is the absolute temperature and R_L is the load resistance. The above noise terms are summarized with considerations of the RIN of the signal light (term no. 1), amplified spontaneous emission (ASE) noise from each EDFA (term no. 2), beat noise between the signal light and the ASE noise (term no. 3), beat noise between ASE components (term no. 4), photon shot noise and thermal noise (term no. 5,6). The DCF module is placed after each optical fiber spool, and loss of each DCF module (7 dB) and SMF spool is just compensated by the optical amplifier. $\langle n_{in} \rangle$ and its corresponding optical power P have the relationship of $e \langle n_{in} \rangle = \Re P$, where \Re is the responsivity of the photodiode. Thus, the SNR of the detected RF signal could be $P_{s-total}/P_{n-total} = 34.4$ dB, which is calculated with $N = 11$, $m = 0.5$, $\Re = 0.8$ A/W, $P = -1$ dBm, $m_t = 2$, $n_{sp} = 2$, $B = 100$ MHz, $n_{RIN} = -120$ dBc/Hz, $\Delta f = 100$ GHz, $T = 296$ K, and $R_L = 50 \Omega$. In our experiment, we measure SNR of the RF signal by using the signal analyzer (ROHDE & SCHWARZ, FSV30). The SNR of 2.4 GHz signal is reduced by ~ 37 dB (@RBW 3 MHz) after transmitted along the 1007 km fiber link which is measured by comparing SNR of signal E_1 with that of the signal E_2 . And the SNR of the received RF signal is 33 dB which is 70 dB before transmission. The theoretical calculation result is better than the measured SNR, which is depending on the actual running status of all the experimental devices. As a consequence, the SNR degradation caused by the long distance transmission is basically consistent with the theoretical calculation result. Besides, the SNR of signal E_4 is improved by 20 dB (@RBW 2 MHz) compared to that generated only by passive frequency mixing. At the LS, the rubidium clock (Quartzlock, A1000) is high stable reference source for frequency synthesizers. As mentioned before, the PDRO is served as ultra low phase noise frequency synthesizer, which comprises a phase detector, low pass filter, divider and dielectric resonant oscillator. Proper electric amplifiers are applied in our system to amplify the electric power of the outputs of mixers. Fig. 2 shows the schematic diagram of the phase noise test. The phases of 2.4 GHz MRF and SRF are compared by an analog double-balanced mixer (Marki M1-0008). Output of this phase comparator passes through a low pass filter(LPF) and the real-time voltage fluctuation of this the DC error signal is collected by a high precision digital multimeter (keysight 34465 A). The output of LPF can be expressed as

$$V(t) = (V_{pp}/2)\cos(\Delta\varphi) + V_o, \tag{11}$$

where $\Delta\varphi$ is residual phase fluctuation of the transmission system, V_o is the inherent DC offset voltage of the analog mixer and V_{pp} is the peak-to-peak voltage of the DC signal $V(t)$. V_{pp} and V_o are measured when the relative phase change between the two mixed signals is greater than 2π . Here, a phase shifter after the MRF is tuned from 0 to 2π to obtain the amplitude information of the DC error signal. The relative phase time fluctuation is calculated by using the function

$$y(t) = (1/f_0 2\pi) \arccos[2(V(t) - V_o)/V_{pp}], \tag{12}$$

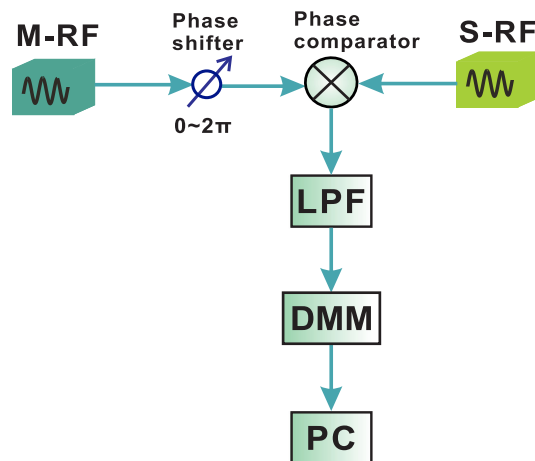


Fig. 2. Schematic diagram of the phase noise test. LPF: low pass filter. DMM: digital multimeter. PC: personal computer.

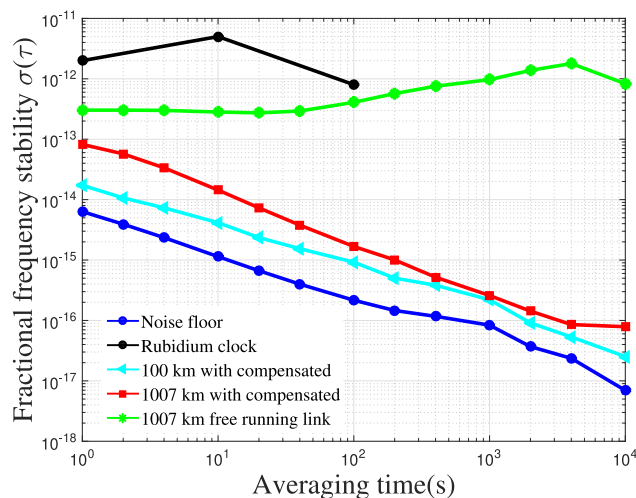


Fig. 3. Fractional frequency instability of the rubidium clock, the 1007 km compensated fiber link and free running link; 100 km compensated fiber link; noise floor of the transmission system.

where f_0 is 2.4 GHz. We calculate the fractional frequency instability (ADEV) of the transfer system by using the phase time fluctuation data. The digits of resolution of the multimeter (keysight 34465 A) is $6^{1/2}$, and this corresponds to ADEV resolution of $\sim 1 \times 10^{-15}$ @1 s. The efficiency of our stabilization system can be observed in Fig. 3. The fractional frequency instability of the free running link is 3.03×10^{-13} @1 s and 8.33×10^{-13} @10 000 s. While the instability of our stabilized system reaches 8.20×10^{-14} @1 s and 7.87×10^{-17} @10 000 s. Noise floor of our system is 6.33×10^{-15} @1 s and 6.95×10^{-18} @10 000 s. The noise floor is obtained by measuring the phase difference between the reference signal generated by MRF and the signal generated by SRF. We use 1 m long SMF to replace the long-haul fiber link, which includes the bi-EDFAs and pre-EDFAs. As for the deterioration of the instability of 1007 km transmission system compared to that of the noise floor, it can be attributed to several asymmetry noise sources. These sources include ASE noise of bi-EDFA, GVD, photon shot noise, amplifier flicker noise, thermal noise, and amplitude-to-phase noise conversion during the photodetection and amplification processes. Fig. 3 also shows the frequency stability of the rubidium clock which is provided by the vendor. The

frequency instability of the rubidium clock provided by vendor comprises only four data values, for averaging times of 1 s, 10 s, 100 s, and 1 d. Because the frequency instability for an averaging time of 1 d is relatively far from 100 s, we could not draw the polyline trend properly. Therefore, we don't give the frequency instability for an averaging time of 1 d in Fig. 3. It should be mentioned that the 1-day fractional frequency stability of the rubidium clock is 8×10^{-12} . We also tested the performance of our system over 100 km underground optical fiber link, ADEV of which is 1.73×10^{-14} @1 s and 2.52×10^{-17} @10 000 s. It can be seen that the short term instability of our RF transmission system is more than an order of magnitude to that of the rubidium clock, which is 2×10^{-12} @1 s. Thus, our high stable RF transfer system has enough ability to transfer this reference signal with minimal degradation of its stability [35]. The good experiment results benefit from the dual-PLL configuration. On the one hand, the two PLLs have low pass filtering characteristics for the long distance transmitted signal, which enhance the sidelobe components of the signal and improve its SNR. On the other hand, PLLs also have the property of high pass filtering of the remarkable OCXO phase noise, which results in better short-term stability of the output signal. The experimental results make it more economical to support long distance RF transmission without substantial instability degradation, and extend the transmission length between cascaded systems.

4. Conclusion

In summary, high stable 2.4 GHz RF signal transfer over 1007 km fiber link is demonstrated without any electric relay system. The fractional frequency instability of the compensated system is 8.20×10^{-14} @1 s and 7.87×10^{-17} @10 000 s. The experiment results prove the validity of our dual-PLL configuration and make the transmission length extended to thousand-kilometer scale. A key outcome of our work is demonstrating RF synchronization with better instability than that of a rubidium clock. This is meaningful for applications requiring long-haul distribution of a local oscillator with low phase drift. Now, the devices of LS and RS have been integrated into two modules and we will carry out more verification experiments of our system in continental underground fiber link. As we look forward to the future of ultrastable long-haul fibre-optic RF transfer, we can come to the realization that this would be essential for establishing continental-scale radio antenna array systems and making cutting-edge discoveries.

References

- [1] P. E. Dewdney, P. J. Hall, R. T. Schilizzi, and T. J. L. Lazio, "The square kilometre array," *Proc. IEEE*, vol. 97, no. 8, pp. 1482–1496, Aug. 2009.
- [2] J.-F. Cliche and B. Shillue, "Applications of control precision timing control for radioastronomy maintaining femtosecond synchronization in the atacama large millimeter array," *IEEE Control Syst. Mag.*, vol. 26, no. 1, pp. 19–26, Feb. 2006.
- [3] E. J. Murphy *et al.*, "Science with an ngVLA: The ngVLA science case and associated science requirements," in *Science with a Next Generation Very Large Array*, vol. 517, pp. 3–14, 2018.
- [4] S. Schediwy *et al.*, "The mid-frequency square kilometre array phase synchronisation system," *Publ. Astron. Soc. Aust.*, vol. 36, Feb. 2019.
- [5] B. Wang *et al.*, "Precise and continuous time and frequency synchronisation at the 5×10^{-19} accuracy level," *Sci. Rep.*, vol. 2, Aug. 2012, Art. no. 556.
- [6] O. Lopez, A. Haboucha, B. Chanteau, C. Chardonnet, A. Amy-Klein, and G. Santarelli, "Ultra-stable long distance optical frequency distribution using the internet fiber network," *Opt. Express*, vol. 20, no. 21, pp. 23518–23526, Oct. 2012.
- [7] P. A. Williams, W. C. Swann, and N. R. Newbury, "High-stability transfer of an optical frequency over long fiber-optic links," *J. Opt. Soc. Amer. B*, vol. 25, no. 8, pp. 1284–1293, Aug. 2008.
- [8] C. Calosso *et al.*, "Frequency transfer via a two-way optical phase comparison on a multiplexed fiber network," *Opt. Lett.*, vol. 39, no. 5, pp. 1177–1180, Mar. 2014.
- [9] X. Chen *et al.*, "Feed-forward digital phase compensation for long-distance precise frequency dissemination via fiber network," *Opt. Lett.*, vol. 40, no. 3, pp. 371–374, Feb. 2015.
- [10] D. R. Gozzard *et al.*, "Astronomical verification of a stabilized frequency reference transfer system for the square kilometre array," *Astron. J.*, vol. 154, no. 1, pp. 1–9, 2017.
- [11] M. Fujieda, M. Kumagai, and S. Nagano, "Coherent microwave transfer over a 204-km telecom fiber link by a cascaded system," *IEEE Trans. Ultrason., Ferroelect., Freq. Control*, vol. 57, no. 1, pp. 168–174, Jan. 2010.
- [12] S. Droste *et al.*, "Optical-frequency transfer over a single-span 1840 km fiber link," *Phys. Rev. Lett.*, vol. 111, no. 11, Sep. 2013, Art. no. 110801.

- [13] O. Lopez *et al.*, "86-km optical link with a resolution of 2×10^{-18} for RF frequency transfer," *Eur. Phys. J. D*, vol. 48, no. 1, pp. 35–41, 2008.
- [14] Ł. Śliwczyński, P. Krehlik, A. Czubla, Ł. Buczek, and M. Lipiński, "Dissemination of time and RF frequency via a stabilized fibre optic link over a distance of 420 km," *Metrologia*, vol. 50, no. 2, pp. 133–145, Feb. 2013.
- [15] Y. He *et al.*, "Long-distance telecom-fiber transfer of a radio-frequency reference for radio astronomy," *Optica*, vol. 5, no. 2, pp. 138–146, Feb. 2018.
- [16] Q. Liu *et al.*, "Simultaneous frequency transfer and time synchronization over a 430 km fiber backbone network using a cascaded system," *Chin. Opt. Lett.*, vol. 14, no. 7, Jul. 2016, Art. no. 070602.
- [17] J. Gao, B. Wang, X. Zhu, Y. Yuan, and L. Wang, "Dissemination stability and phase noise characteristics in a cascaded, fiber-based long-haul radio frequency dissemination network," *Rev. Sci. Instrum.*, vol. 86, no. 9, Sep. 2015, Art. no. 093111.
- [18] J. Shen, G. Wu, L. Hu, W. Zou, and J. Chen, "Active phase drift cancellation for optic-fiber frequency transfer using a photonic radio-frequency phase shifter," *Opt. Lett.*, vol. 39, no. 8, pp. 2346–2349, Apr. 2014.
- [19] M. Jiang *et al.*, "Multi-access RF frequency dissemination based on round-trip three-wavelength optical compensation technique over fiber-optic link," *IEEE Photon. J.*, vol. 11, no. 3, Jun. 2019, Art. no. 7202808.
- [20] L. Yu *et al.*, "WDM-based radio frequency dissemination in a tree-topology fiber optic network," *Opt. Exp.*, vol. 23, no. 15, pp. 19783–19792, Jul. 2015.
- [21] J. Wei, F. Zhang, Y. Zhou, D. Ben, and S. Pan, "Stable fiber delivery of radio-frequency signal based on passive phase correction," *Opt. Lett.*, vol. 39, no. 11, pp. 3360–3362, Jun. 2014.
- [22] W. Li, W. Wang, W. Sun, W. Wang, and N. Zhu, "Stable radio-frequency phase distribution over optical fiber by phase-drift auto-cancellation," *Opt. Lett.*, vol. 39, no. 15, pp. 4294–4296, Aug. 2014.
- [23] R. Huang, G. Wu, H. Li, and J. Chen, "Fiber-optic radio frequency transfer based on passive phase noise compensation with frequency dividing and filtering," *Opt. Lett.*, vol. 41, no. 3, pp. 626–629, Feb. 2016.
- [24] C. Liu *et al.*, "GVD-insensitive stable radio frequency phase dissemination for arbitrary-access loop link," *Opt. Exp.*, vol. 24, no. 20, pp. 23376–23382, Oct. 2016.
- [25] B. Ning, S. Zhang, D. Hou, J. Wu, Z. Li, and J. Zhao, "High-precision distribution of highly stable optical pulse trains with 8.8×10^{-19} instability," *Sci. Rep.*, vol. 4, May 2014, Art. no. 5109.
- [26] N. Deng, Z. Liu, X. Wang, T. Fu, W. Xie, and Y. Dong, "Distribution of a phase-stabilized 100.02 ghz millimeter-wave signal over a 160 km optical fiber with 4.1×10^{-17} instability," *Opt. Exp.*, vol. 26, no. 1, pp. 339–346, Jan. 2018.
- [27] S. M. Foreman, K. W. Holman, D. D. Hudson, D. J. Jones, and J. Ye, "Remote transfer of ultrastable frequency references via fiber networks," *Rev. Sci. Instrum.*, vol. 78, no. 2, Feb. 2007, Art. no. 021101.
- [28] L. E. Primas, R. T. Logan, and G. F. Lutes, "Applications of ultra-stable fiber optic distribution systems," in *Proc. 43rd Annu. Symp. Freq. Control*, 1989, pp. 202–211.
- [29] Ł. Śliwczyński and J. Kołodziej, "Bidirectional optical amplification in long-distance two-way fiber-optic time and frequency transfer systems," *IEEE Trans. Instrum. Meas.*, vol. 62, no. 1, pp. 253–262, Jan. 2013.
- [30] M. Amemiya, M. Imae, Y. Fujii, T. Suzuyama, and S.-i. Ohshima, "Simple time and frequency dissemination method using optical fiber network," *IEEE Trans. Instrum. Meas.*, vol. 57, no. 5, pp. 878–883, May 2008.
- [31] S. Pan, J. Wei, and F. Zhang, "Passive phase correction for stable radio frequency transfer via optical fiber," *Photon. Netw. Commun.*, vol. 31, no. 2, pp. 327–335, Apr. 2016.
- [32] C. Liu *et al.*, "Ultrastable long-haul fibre-optic radio frequency transfer based on PLL frequency mixing," in *Proc. Joint Conf. IEEE Int. Freq. Control Symp. Int. Symp. Appl. Ferroelect.*, 2020, pp. 1–2.
- [33] F. Narbonneau *et al.*, "High resolution frequency standard dissemination via optical fiber metropolitan network," *Rev. Sci. Instrum.*, vol. 77, no. 6, Jun. 2006, Art. no. 064701.
- [34] S. Shimada and H. Ishio, *Optical Amplifiers and Their Applications*. Hoboken, NJ: Wiley, 1994.
- [35] L. E. Primas, G. F. Lutes, and R. L. Sydnor, "Stabilized fiber-optic frequency distribution system," *Telecommun. Data Acquis. Prog. Rep.*, pp. 88–97, 1989.